ISSN 0005–1144
ATKAAF 42(1–2), 29–36 (2001)

Ján Vittek, Stephen J. Dodds, Juraj Altus, Roy Perryman

Vector-Controlled Reluctance Synchronous Motor Drives with Prescribed Closed-Loop Speed Dynamics

UDK 621.313.323
IFAC IA 5.5.4;4.7.1

Original scientific paper

A new speed control system for electric drives employing reluctance synchronous motors is presented. Design control system combines two control methods. Conventional vector control method is here completed with forced dynamics closed-loop control. Since the closed-loop system response is a first order lag whose pole location can be chosen by the user, the drive may be included as an actuator in a larger scale control scheme to which linear control system design methods can be applied. To improve robustness of the design control structure, the outer control loop based on model reference adaptive control is added. Simulation results presented show good correspondence with theoretical predictions and MRAC outer control loop improves overall drive performances.

Key words: linearisation, model reference adaptive control, non-linear system control, observers, reluctance synchronous motor, sliding-mode control

1. INTRODUCTION

In contrast to conventional approaches to electric drives a new control strategy for reluctance synchronous motors (*RSM*) is presented. The combined RSM and load are viewed as a multivariable plant, the *control* variables, *measurement* variables and *controlled* variables being, respectively, the *dc circuit voltage*, *the stator currents*, and *the rotor position*. *The non-linear control law which employs RSM vector control* [1], *generates automatically* such stator current demands that rotor speed achieves prescribed closed-loop dynamics. The strategy embodies the block control principle [2], the motion separation principle [3] and sliding mode control [4], the combination of which forms a new non-linear multivariable control method.

The design system comprises two parts: a) the control law comprising *master* and *slave* control laws arranged in a hierarchical structure [2] and b) the state estimation and filtering system, comprising a complementary set of two observers, one used for reconstruction of the rotor speed, and the other for

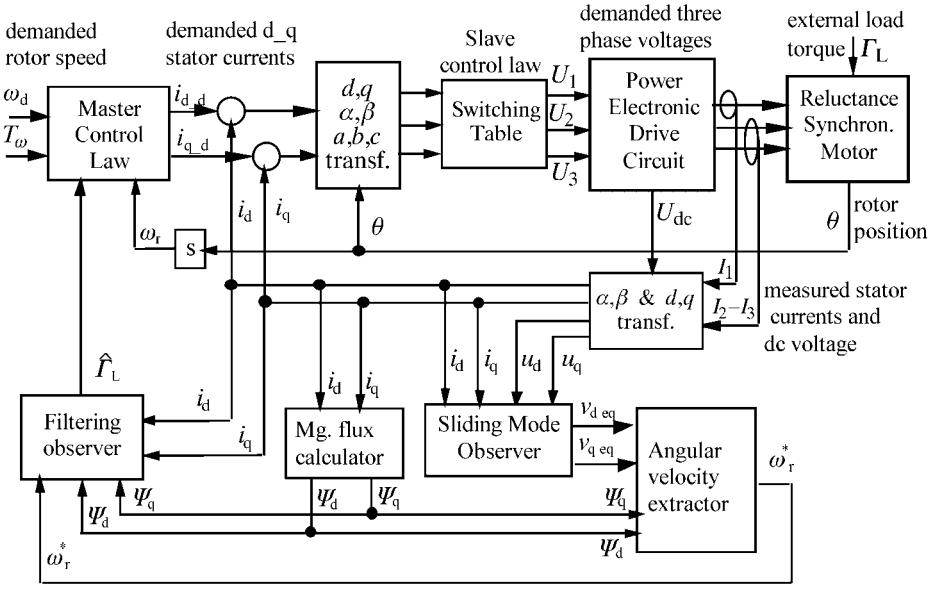

Fig. 1 Overall control system blosk diagram

external torque estimation [5]. Figure 1 shows the control system structure and its operation, the individual blocks being fully explained in the following sections.

The same approach has also been investigated for permanent magnet synchronous motor drives [5, 6] and preliminary experimental results were presented in [7, 8]. The rotor speed is controlled with linear, first order closed-loop dynamics, where the closed-loop time constant can be chosen by the control system designer. In this initial investigation, the RSM motor is assumed to drive a rigid body inertial load with moment of inertia, J and subject to a constant external load torque, Γ_L.

2. CONTROL SYSTEM DEVELOPMENT

2.1. Model of Motor and Load

The following set of non-linear differential equations formulated in the rotating d-q co-ordinate system, coupled to the rotor, describe the RSM and form the basis of the control system development:

$$\boldsymbol{u}_s = R_s \boldsymbol{i}_s + \frac{\mathrm{d}}{\mathrm{d}t}\Psi_s + j\omega_r \Psi_s \tag{2.1}$$

$$T_d = \frac{3p}{2}(\Psi_d i_q - \Psi_q i_d) - \Gamma_L = c_5(L_d - L_q) i_d i_q - \Gamma_L \tag{2.2}$$

where $\boldsymbol{i}_s = i_d + j i_q$, $\boldsymbol{u}_s = u_d + j u_q$ and $\Psi_s = \Psi_d + j\Psi_q$ are, respectively, the stator current, voltage components and magnetic flux components, ω_r is the rotor velocity, p is number of stator pole pairs, Γ_L is the external load torque, R_s is the phase resistance, L_d and L_q are the direct and quadrature phase inductances and constant $c_5 = 3p/2$. The ALA RSM parameters assumed in this study are listed an the Appedix. For its magnetic flux components is valid $\Psi_d = L_d(i_d) \cdot i_d$ and $\Psi_q = L_q \cdot i_q$.

2.2. Master Control Law

The basic philosophy in the control law development is in conjunction with vector control law approach the formulation of *linearising functions* which force a nonlinear system to obey specified linear closed-loop differential equations, which may be of first order yielding a dynamic response to a demanded angular velocity, $\omega_d(t)$, with a prescribed time constant, T_ω. The rotor speed therefore is made to satisfy:

$$\frac{\mathrm{d}\omega_r}{\mathrm{d}t} = \frac{1}{T_\omega}(\omega_d - \omega_r). \tag{2.3}$$

The rotor speed linearising function is chosen to force the non-linear differential equation (2.2) to have the same response as the linear equation (2.3). The linearising function is obtained simply by equating the right hand sides of (2.2) and (2.3), as follows:

$$\frac{1}{J}\left[c_5(\Psi_d i_q - \Psi_q i_d) - \Gamma_L\right] = \frac{1}{T_\omega}(\omega_d - \omega_r). \tag{2.4}$$

In the control law to be derived, estimates of the magnetic flux components, Ψ_d and the Ψ_q are evaluated from the known stator currents, i_d and i_q, by the magnetic flux calculator which takes into account value of direct inductance, L_d as a function of current in direct axis, i_d, (*see Appendix*) while quadrature inductance, L_q, is taken as a constant:

$$_d = L_d(i_d) \cdot i_d \quad \text{and} \quad \Psi_q = L_q i_q \,. \tag{2.5}$$

The second part of the control law is formulated on the basis of vector control [1], which requires for maximum torque for a given flux constant i_d current component up to base speed not to allow its reduction under prescribed value for idle running RSM.

$$\begin{aligned} i_d &= i_{dK} \quad \text{for} \quad \omega_r \langle \omega_{\text{base}} \\ i_d &= i_{dK} \frac{\omega_{\text{base}}}{|\omega_r|} \quad \text{for} \quad \omega_r \rangle \omega_{\text{base}} \,. \end{aligned} \tag{2.6a}$$

For maximum power factor stator current, i_d, can be determined as:

$$i_d = \sqrt{\frac{\frac{J}{T_\omega}(\omega_d - \omega_r) + \Gamma_L}{c_5(L_d - L_q)\tan\delta}}. \tag{2.6b}$$

Equations (2.4) and (2.6) are now solved for corresponding i_q. The expressions obtained are then used to generate the *demanded* values of i_d and i_q which will be denoted respectively by i_{d_d} and i_{q_d}. Thus, using the flux estimates from equation (2.5), and load torque estimate, $\hat{\Gamma}_L$, from the observer of section 3, the following master control laws are derived:

a) with respect of maximum torque per given flux:

$$\begin{aligned} i_{d\_d} &= i^*_{dK} \\ i_{q\_d} &= \frac{\frac{J}{T_\omega}(\omega_d - \omega_r) + \Gamma_L}{c_5(L_d - L_q)\, i^*_{dK}} \end{aligned} \tag{2.7a}$$

b) with respect of maximum power factor:

$$\begin{aligned} i_{d\_d} &= \sqrt{\frac{\left|\frac{J}{T_\omega}(\omega_d - \hat{\omega}_r) + \hat{\Gamma}_L\right|}{c_5\left(\tilde{L}_d - \tilde{L}_q\right)\tan(\delta)}}, \\ i_{q\_d} &= i_{d\_d} \tan(\delta) \cdot \mathrm{sgn}\left(T_d\right). \end{aligned} \tag{2.7b}$$

The estimates of all constant parameters, p, used in any model-based control law cannot be known with infinite precision, and therefore they were denoted by $\tilde{p}$.

2.3. The Slave Control Law

The sub-plant to be controlled here is defined by equation (2.1), the control variables now being u_d and u_q and the output variables i_d and i_q to respond to the demanded currents i_{d_d} and i_{q_d}. The slave control law is the following *bang-bang control law*:

$$u_j = U_s \operatorname{sgn}(i_{j\_d} - i_j), \quad j = 1, 2, 3. \tag{2.8}$$

Generally the transformations between the *d-q* components of the stator currents and voltages and the corresponding three-phase stator voltages and currents are given by:

$$\begin{bmatrix} z_d \\ z_q \end{bmatrix} = \begin{bmatrix} C & S \\ -S & C \end{bmatrix} \cdot \begin{bmatrix} 2/3 & -1/3 & -1/3 \\ 0 & 1/\sqrt{3} & -1/\sqrt{3} \end{bmatrix} \cdot \begin{bmatrix} z_1 \\ z_2 \\ z_3 \end{bmatrix} \tag{2.9}$$

where: $C = \cos(\omega_r t)$ and $S = \sin(\omega_r t)$.

Special starting algorithm with constant current i_d and i_q demands comes into play while minimal magnetic flux norm isn't built. To simplify calculations, magnetic flux norm has definition:

$$\|\Psi\| = \Psi_d^2 + \Psi_q^2 . \tag{2.10}$$

3. STATE ESTIMATION AND FILTERING

The load torque, which is necessary for master control algorithm, is gained similar way to that of [4] and [5] for synchronous motor. First, a stator current vector *pseudo sliding-mode* observer is formulated for generation of an unfiltered estimate of rotor speed. The load torque estimate required by the master control law is provided in second step by a standard observer having a similar structure to a Kalman filter, a direct measurement of load torque being assumed to be unavailable.

3.1. The pseudo sliding mode observer and angular velocity extractor

The real time model of the system done by stator currents equation (3.1) fed by actual stator voltages and real stator currents is developed but *purposely using only the terms without rotor speed*, ω_r. Thus:

$$\frac{\mathrm{d}}{\mathrm{d}t}\begin{bmatrix} i_d^* \\ i_q^* \end{bmatrix} = \begin{bmatrix} \frac{1}{\tilde{L}_d} & 0 \\ 0 & \frac{1}{\tilde{L}_q} \end{bmatrix} \cdot \begin{bmatrix} u_d \\ u_q \end{bmatrix} - \begin{bmatrix} \frac{R_s}{L_d} & 0 \\ 0 & \frac{R_s}{L_q} \end{bmatrix} \cdot \begin{bmatrix} i_d \\ i_q \end{bmatrix} + \begin{bmatrix} v_{\mathrm{eq}d} \\ v_{\mathrm{eq}q} \end{bmatrix} \tag{3.1}$$

where $v_{\mathrm{eq}d}$ and $v_{\mathrm{eq}q}$ are the model corrections and i_d^* and i_q^* are estimates of i_d and i_q as in a conventional observer. The useful observer outputs here are the continuous *equivalent values* of the rapidly switching variables:

$$\begin{bmatrix} v_{\mathrm{eq}d} \\ v_{\mathrm{eq}q} \end{bmatrix} = V_{\max} \operatorname{sgn}\begin{bmatrix} i_d & -i_d^* \\ i_q & -i_q^* \end{bmatrix}. \tag{3.2}$$

Equation (3.2) cannot directly generate $v_{\mathrm{eq}d}$ and $v_{\mathrm{eq}q}$. Instead, a *pseudo-sliding-mode* observer may be formed by replacing equation (3.2) with (3.3):

$$\begin{bmatrix} v_{\mathrm{eq}d} \\ v_{\mathrm{eq}q} \end{bmatrix} = K_{\mathrm{sm}} \begin{bmatrix} i_d & -i_d^* \\ i_q & -i_q^* \end{bmatrix} \tag{3.3}$$

where the gain, K_{sm}, is made as high as possible within the stability limit. For large K_{sm}, the errors between real motor currents and fictitious observer currents are driven almost to zero with the result yielding (3.4):

$$\begin{bmatrix} v_{\mathrm{eq}d} \\ v_{\mathrm{eq}q} \end{bmatrix} = \begin{bmatrix} 0 & p\omega_r^* \frac{\tilde{L}_q}{\tilde{L}_d} \\ -p\omega_r^* \frac{\tilde{L}_d}{\tilde{L}_q} & 0 \end{bmatrix} \cdot \begin{bmatrix} i_d \\ i_q \end{bmatrix}. \tag{3.4}$$

Based on equation (3.4) an unfiltered angular rotor velocity estimate, ω_r^*, can be extracted. The component, $v_{\mathrm{eq}q}$ of (3.4), which has minimal noise distortion, was used for extraction of angular speed estimate. Special correction algorithm is used for additional filtering of pseudo-sliding mode observer output.

$$\omega_r^* = \frac{-\tilde{L}_q v_{\mathrm{eq}q}}{p\tilde{L}_d i_d} . \tag{3.5}$$

3.2. The load torque observer

There is no direct means of measuring the external load torque, Γ_L. This problem is easily solved, however, by treating Γ_L as a state variable and including its estimate in the real time model of an observer. If the stator current measurement noise is significant, then the system performance will be improved by using the angular velocity estimate, $\hat{\omega}_r$, from the observer, which is a *filtered* version of ω_r^*. The observer presented produces this filtered angular velocity estimate without impairing the control system performance by introduction of a dynamic lag, in a similar fashion to a Kalman filter. The combined rotor speed and load torque for control algorithm is then observed.

The real time model of this observer is based on torque equations (2.2). The observer correction

loop is actuated by the error between the rotor speed estimate, ω_r^*, from the angular velocity extractor of previous section and the estimate, $\hat{\omega}_r$, from the real time model.

$$e_\omega = \omega_r^* - \hat{\omega}_r$$

$$\dot{\hat{\omega}}_r = \frac{1}{\tilde{J}}\left(\frac{3p}{2}\left[\left(\Psi_d i_q - \Psi_q i_d\right) - \hat{\Gamma}_L\right]\right) + k_\omega e_\omega \quad (3.6)$$

$$\dot{\hat{\Gamma}}_L = k_\Gamma e_\omega .$$

Since $\hat{\omega}_r$ is a filtered version of ω_r^* it is used directly in the master control law. This is a conventional second order linear observer with a correction loop characteristic polynomial, which may be chosen via the gains, k_ω and k_Γ, to yield the desired balance of filtering between the noise from the measurements of currents i_d and i_q and the noise from the velocity measurement, ω_r^*.

4. MODEL REFERENCE BASED CONTROL LAW

To improve derived control law an alternative simple Model Reference Adaptive Control (*MRAC*) is designed. The purpose of it is to form a real time model of the ideal closed-loop system and »*slave*« the plant to follow this by means of a high gain correction loop, as shown in Figure 2.

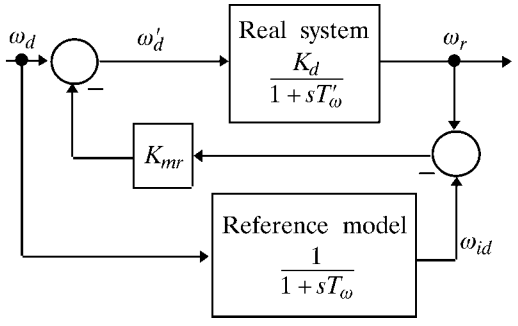

Fig. 2 Model reference based outer control loop

Since the middle loop controller is model based (as it was mentioned, it contains algorithms depending on estimates of the motor and load parameters) the closed-loop performance will be affected by the errors in these estimates. It is also clear that an un-modelled external load torque, Γ_L, will also affect the closed-loop performance. Let the errors introduced by the motor parameter uncertainties, external load torque and imperfect operation of the middle control loop due to the non-zero iteration interval be (roughly) represented by a change of time constant and DC gain. Then the transfer function of real system, formed by the inner and middle control loop is of the following form:

$$\frac{\hat{\omega}_r(s)}{\omega_d'(s)} = \frac{K_d}{1+sT_\omega'}. \quad (4.1)$$

The purpose of the outer loop controller is to improve the robustness of the overall control system against uncertain parameters and external load torque. Outer control loop controller is a MRAC based. This model is governed by transfer function (4.2):

$$\frac{\hat{\omega}_r(s)}{\omega_d'(s)} = \frac{1}{1+sT_\omega}. \quad (4.2)$$

Thus, the demanded angular velocity, ω_d', is applied to the reference model and to the closed-loop system formed by the original controller with inner and middle loop. Any mismatch between the real system and the closed-loop reference model then gives rise to a correction, $K_{mr}\cdot(\hat{\omega}_r - \omega_{id})$, applied to the real system to force it to follow the model. As the model reference control loop gain, K_{mr}, is increased, then, in theory, the error, $(\hat{\omega}_r - \omega_{id})$, is reduced, thereby causing the real system to be »slaved« to the model. Applying Mason's formula to the Figure 2 yields:

$$\frac{\hat{\omega}_r(s)}{\omega_d(s)} = \frac{\frac{K_d}{1+sT_\omega'}\left(1 + K_{mr}\frac{1}{1+sT_\omega}\right)}{1+\left(K_{mr}\frac{K_d}{1+sT_\omega'}\right)}. \quad (4.3)$$

Thus, as K_{mr}, tends to infinity, transfer function between estimated speed and demanded speed tends to the demanded transfer function (4.2), predicting the required robustness.

$$\frac{\hat{\omega}_r(s)}{\omega_d(s)} \to \frac{1}{1+sT_\omega} \quad \text{for} \quad K_{mr} \to \infty . \quad (4.4)$$

In practice, however, K_{mr} will be limited by any un-modelled plant dynamics and the non-zero iteration interval. A shortfall in robustness would still be expected since the system depends on the accuracy of the speed estimate, $\hat{\omega}_r$.

5. VERIFICATION BY SIMULATION

All the simulation results are presented in Figure 3, Figure 4, Figure 5 and Figure 6. They were carried out with computational step $\Delta t = 5e-5s$, which corresponds to the sampling interval 20 kHz for digital implementation.

The response of the basic control system with the control laws designed by equations (2.7a) and (2.7b) are simulated the first to illustrate the operation of a new vector controlled RSM drive with forced dynamic. These results are shown in the Figure

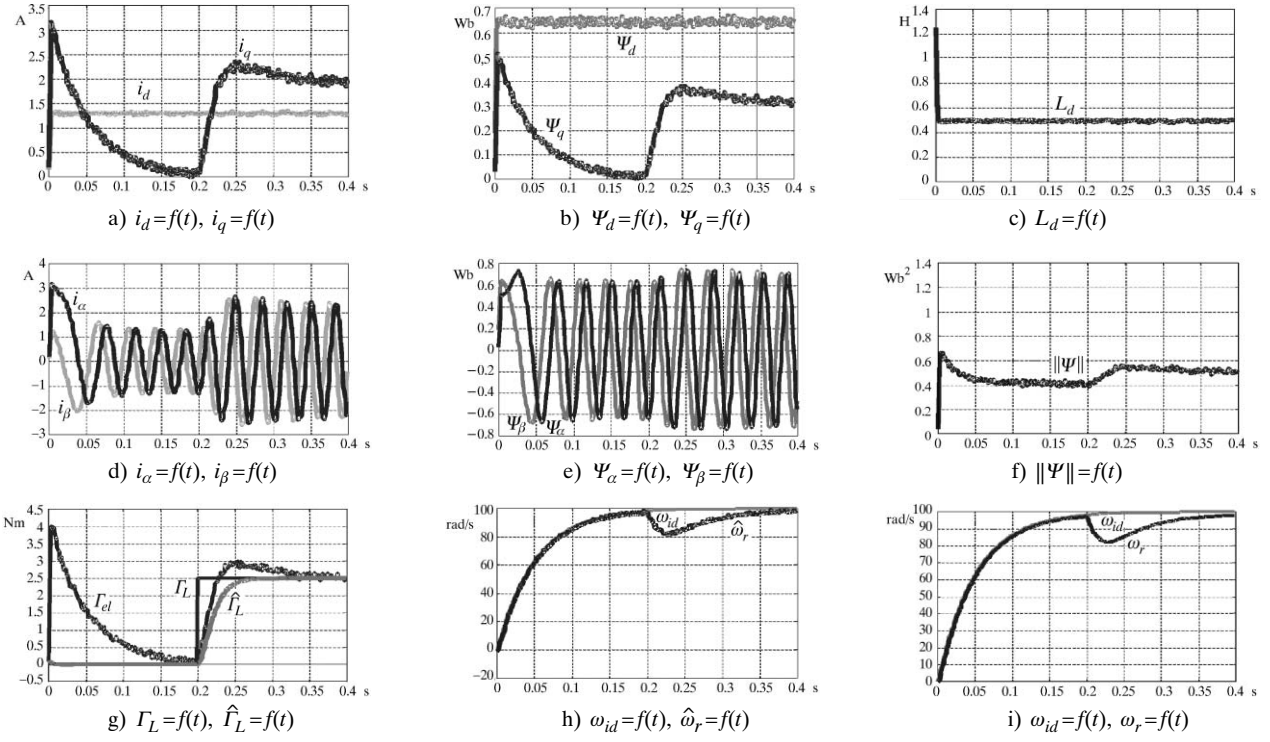

a) $i_d=f(t)$, $i_q=f(t)$ b) $\Psi_d=f(t)$, $\Psi_q=f(t)$ c) $L_d=f(t)$

d) $i_\alpha=f(t)$, $i_\beta=f(t)$ e) $\Psi_\alpha=f(t)$, $\Psi_\beta=f(t)$ f) $\|\Psi\|=f(t)$

g) $\Gamma_L=f(t)$, $\hat{\Gamma}_L=f(t)$ h) $\omega_{id}=f(t)$, $\hat{\omega}_r=f(t)$ i) $\omega_{id}=f(t)$, $\omega_r=f(t)$

Fig. 3 Forced dynamic vector control of RSM with maximum torque for a given flux

3 for maximum torque per given flux ($i_d=\text{const}$) and in Figure 5 for maximum power factor. The results are then compared with corresponding responses of a control system employing the MRAC based outer control loop what is shown in the Figure 4 and Figure 5.

In all presented figures the subplots (a) and (b) show demanded and real values of current components and real values of magnetic flux component in the d_q rotor fixed frame. Changes of direct inductance, L_d due to changes of direct current, i_d, are shown in the subplot (c). The subplot (d) and (e) show the stator currents and magnetic flux components viewed in the stator fixed α_β frame. Subplot (f) shows magnetic flux norm as it was defined by equation (2.10) as a function of time. Subplot (g) shows the initially exponentially decaying electrical torque from the motor, applied load torque, Γ_L together with its estimate $\hat{\Gamma}_L$ from filtering observer. The estimated values of load torque from the observer may just be seen to follow the step increase in load torque at $t=0.2$ s with a small dynamic lag according to $T_{s0}=50$ ms. This gives rise to the small transient reduction in the rotor speed just after $t==$ 0.2 s. Speed estimate from filtering observer together with ideal speed response are shown in the subplot (h). Finally subplot (i) shows ideal speed response and real rotor speed as a function of time.

The control law parameters for all simulations are as follows: master control law closed-loop time constant: $T_\omega=0.05$ s; observer filtering time constant: $T_{s0}=0.05$ s; pseudo sliding mode observer model correction loop gain: $K_{sm}=16\,000$. In all these simulations perfect matching conditions between the motor parameters and those assumed in the control laws and observers are assumed.

Apart from the transient due to small lag in load torque estimation, the required first order dynamic with a prescribed time constant of $T_\omega=0.05$ s is evident if real motor speed is compared with ideal one (Figure 3i and Figure 4i) for both way of RSM vector control.

Substantial improvement of the drive performance for both control algorithms can be seen when MRAC outer loop is added (Figure 5 and Figure 6). While compensation of the angular speed drop due to application of nominal load torque takes approximately 0.2 s for basic algorithms, this is compensated in 0.05 s when MRAC outer control loop is added. Also the absolute value of speed drop is nearly four times lower for MRAC algorithms (Figure 5i and Figure 6i) if it is compared with standard vector algorithms (Figure 3i and Figure 4i).

As an evaluation of the presented simulations it is possible to conclude that application of MRAC based outer control loop substantially improves be-

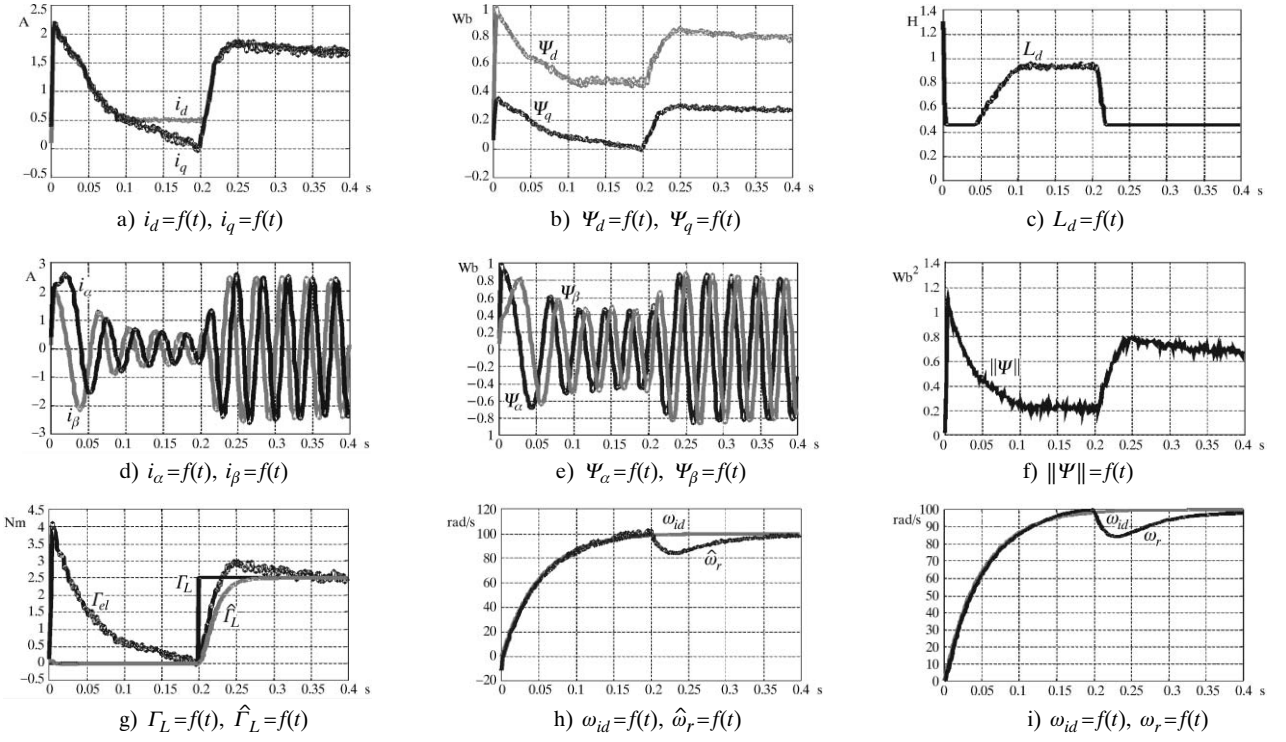

a) $i_d=f(t)$, $i_q=f(t)$ b) $\Psi_d=f(t)$, $\Psi_q=f(t)$ c) $L_d=f(t)$

d) $i_\alpha=f(t)$, $i_\beta=f(t)$ e) $\Psi_\alpha=f(t)$, $\Psi_\beta=f(t)$ f) $\|\Psi\|=f(t)$

g) $\Gamma_L=f(t)$, $\hat{\Gamma}_L=f(t)$ h) $\omega_{id}=f(t)$, $\hat{\omega}_r=f(t)$ i) $\omega_{id}=f(t)$, $\omega_r=f(t)$

Fig. 4 Forced dynamic vector control of RSM with maximum pover factor

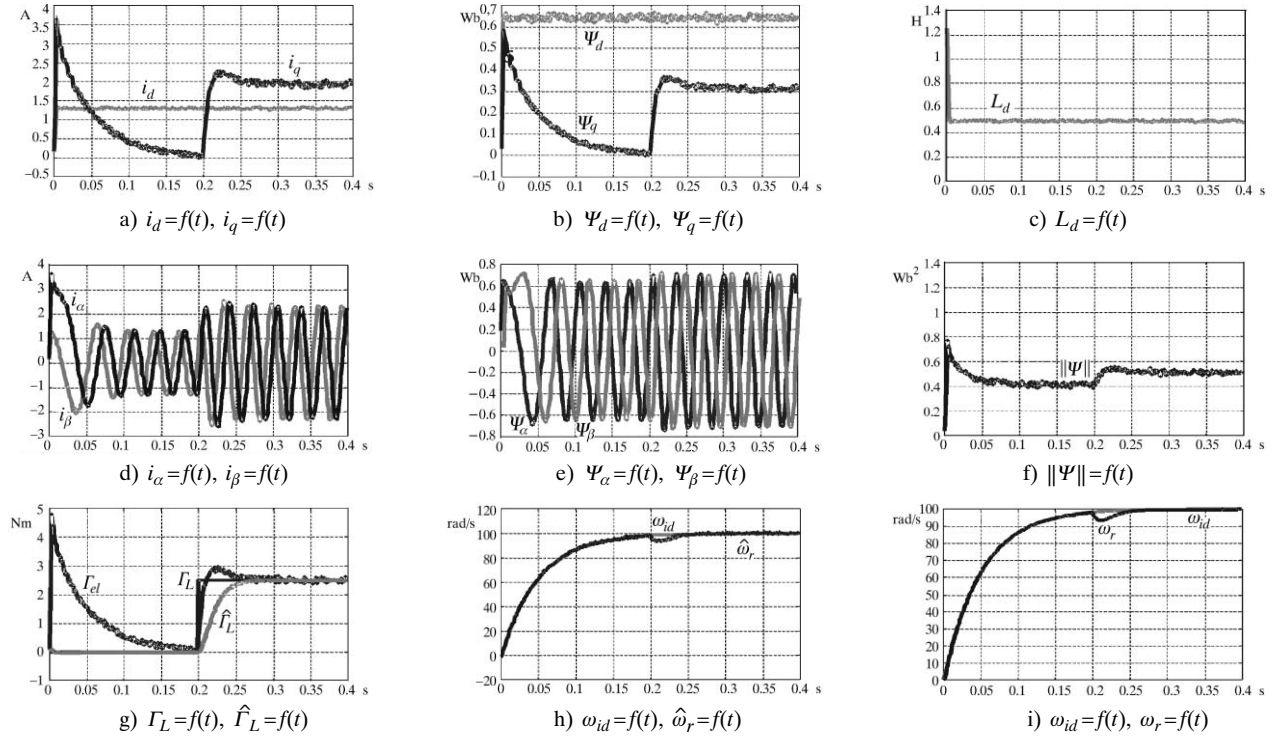

a) $i_d=f(t)$, $i_q=f(t)$ b) $\Psi_d=f(t)$, $\Psi_q=f(t)$ c) $L_d=f(t)$

d) $i_\alpha=f(t)$, $i_\beta=f(t)$ e) $\Psi_\alpha=f(t)$, $\Psi_\beta=f(t)$ f) $\|\Psi\|=f(t)$

g) $\Gamma_L=f(t)$, $\hat{\Gamma}_L=f(t)$ h) $\omega_{id}=f(t)$, $\hat{\omega}_r=f(t)$ i) $\omega_{id}=f(t)$, $\omega_r=f(t)$

Fig. 5 Forced dynamic vector control of RSM with maximum torque for a given flux and MRAC based outer control loop

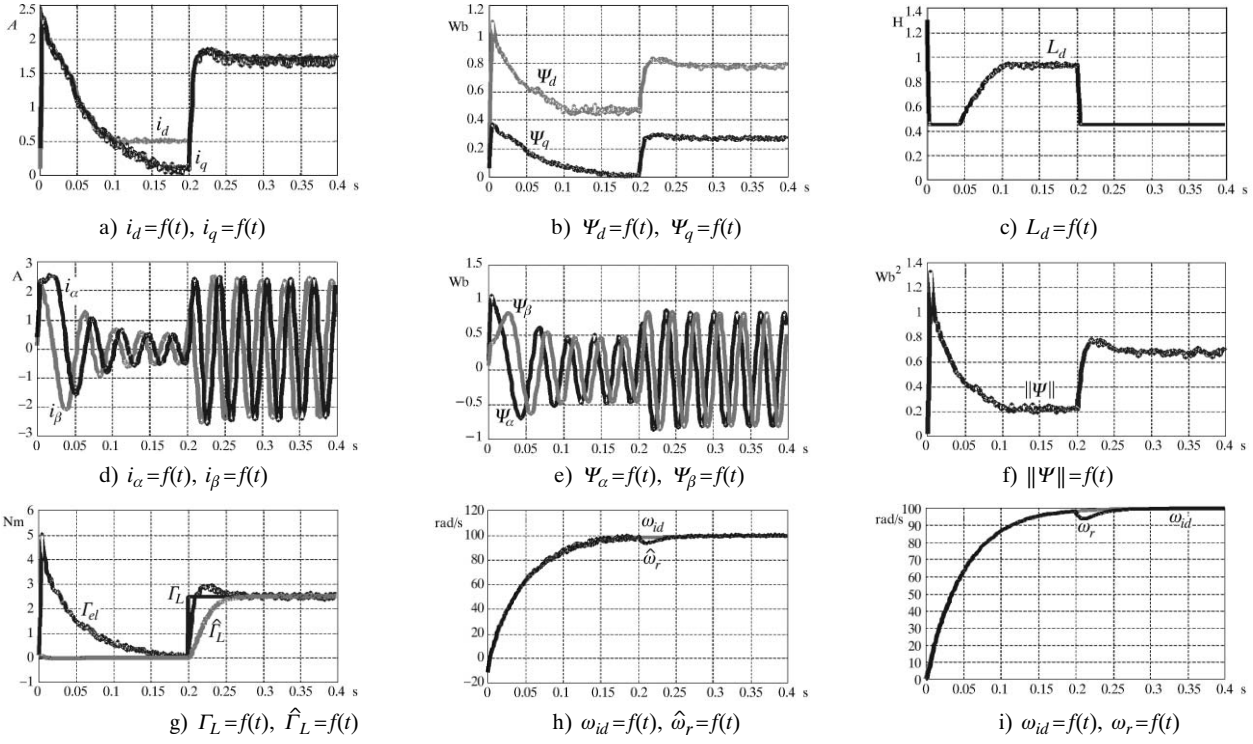

Fig. 6 Forced dynamic vector control of RSM with maximum torque per stator current and MRAC outer control loop

havior of the drive with SRM. The significant reduction of the error between ideal speed response computed from transfer function and real rotor speed brought about by the MRAC outer control loop is evident by comparison of corresponding Figure 3 and Figure 5 for maximum torque per given flux control and Figure 4 and Figure 6 for maximum torque per stator current control.

6. CONCLUSIONS

The simulation results of the proposed new control method for electric drives employing RSM with forced dynamics show a good agreement with the theoretical predictions. The only substantial departure of the system performance from the ideal is the transient influence of the external load torque on the demanded rotor speed. Although this effect is not too serious, a means of reducing it with MRAC outer control loop were verified.

Some preliminary investigations to test the robustness to motor parameter mismatches show promising results which are not published here due to space limitations mainly if MRAC outer control loop is added. Further investigations of robustness, however, should be carried out, particularly with regard to dynamic load parameter mismatches and time varying external load torque. It is highly desirable to employ suggested control strategy also experimentally with a new ALA RSM described in [9].

REFERENCES

[1] I. Boldea, A. S. Nasar, **Vector Control of AC Drives.** CRC Press London, United Kingdom, 1992.

[2] S. V. Drakunov, D. B. Izosimov, A. G. Lukyanov, V. A. Utkin, V. I. Utkin, **The Block Control Principle, I, II.** Automation and Remote Control, vol. 45, no. 5, pp. 601–609, May 1990.

[3] V. I. Utkin, **Method of Separation of Motions in Observation Problems.** Automation and Remote Control, vol. 44, no. 12, pp. 300–308, Dec. 1990.

[4] V. I. Utkin, **Sliding Modes in Control and Optimisation.** Springer-Verlag Berlin, Germany, 1992.

[5] S. J. Dodds, V. A. Utkin, J. Vittek, **Self Oscillating, Synchronous Motor Drive Control System with Prescribed Closed--Loop Speed Dynamics.** Proc. 2nd EPE Chapter Symp., pp. 23–28, Nancy, France, June 1996.

[6] S. J. Dodds, J. Vittek, **Synchronous Motor Drive with Prescribed Closed-Loop Speed Dynamics Employing A Two--Phase Oscillator.** Proc. EDPE'96 Conf., vol. 1, pp. 80–88, High Tatras, Slovakia, Oct. 1996.

[7] S. J. Dodds, J. Vittek, S. Seman, **Implementation of a Sensorless Synchronous Motor Drive Control System with Prescribed Closed-Loop Speed Dynamics.** Proc. SPEEDAM'98 Symp., pp. P4-5–P4-10, Sorrento, Italy, June 1998.

[8] J. Vittek, J. Altus, S. J. Dodds, R. Perryman, **Preliminary Experimental Results for Synchronous Motor Drive with Forced Dynamics.** Proc. IASTED'98 »Control and Applications« Conf., pp. 219–223, Honolulu, USA, August 1998.

[9] M. Licko, V. Hrabovcova, **Design Aspects of Axially Laminated Anisotropic (ALA) Reluctance Synchronous Motor.** Proc. Transcom'99 University of Zilina Conf., vol. 3, pp. 39–45, Slovakia, May 1999.

Appendix

Reluctance synchronous motor parameters			
Nominal voltage	380 V (for Y)	Stator resistance	$R_s = 8.62\ \Omega$
Nominal current	2.01 A	Quadr. inductance	$L_q = 161.8$ mH
Rated power	400 W	Number of polpairs	$p = 2$
Inverter dc voltage	550 V	Moment of inertia	$J = 0.0021$ kgm^2

Polynomial approximation of the direct inductance $L_d(i_d)$ in the working range of stator currents:
$L_d = 0.2913 \cdot i_d^2 - 1.0755 \cdot i_d + 1.4$ H; A
with condition:
if $L_d < 0.45$ then $L_d = 0.45$.

Acknowledgements

The authors wish to thank the *Slovak Grant Agency VEGA* for funding research programme No.106/603, which enabled us to present these results.

Vektorski upravljani elektromotorni pogoni s reluktantnim sinkronim motorima uz definiranu dinamiku zatvorenog kruga brzine vrtnje. Prikazana je nova koncepcija sustava upravljanja brzinom vrtnje elektromotornog pogona s reluktantnim sinkronim motorima, temeljena na dvijema metodama upravljanja. Konvencionalna vektorska metoda nadograđena je elementom sustava koji predstavlja dinamiku zatvorenog kruga po brzini vrtnje. Budući da je dinamika zatvorenog sustava prikazana proporcionalnim članom prvog reda, čiji pol odabire korisnik, predložena koncepcija može biti šire primjenjiva. Da bi se poboljšala robusnost sustava, dodana je vanjska petlja upravljanja zasnovana na adaptivnom upravljanju s referentnim modelom. Simulacijski rezultati prikazani u radu potvrđuju valjanost predložene koncepcije.

Ključne riječi: linearizacija, adaptivno upravljanje s referentnim modelom, nelinearni sustav upravljanja, estimator, reluktantni sinkroni motor, klizni režimi

AUTHORS' ADDRESSES:

Prof. Ing. Ján Vittek, PhD.
Assoc. Prof. Ing. Juraj Altus, PhD.
University of Zilina
Department of Electric Traction and Energetic
010 26 Zilina, Slovak Republic

Prof. Stephen James Dodds
Dr. Roy Perryman
University of East London,
School of Electrical and Manufacturing Engineering
Dagenham, Essex, RM8 2AS, United Kingdom

Received: 2001–10–05